Elastic Hadron Scattering & Alan Krisch

Cornell & Michigan

1963 - 1971

Carl W. Akerlof

University of Michigan

Elastic scattering cross sections

(all variables are in the C-M frame)

Kinematics:

$$|\mathbf{q}| = |\mathbf{p}_f - \mathbf{p}_i| = 2\,p_{CM} \sin\left(\frac{\theta}{2}\right) = \sqrt{-t}$$

$$p_\perp = p_{CM}\ \sin\,(\theta_{CM}) = 2\ p_{CM}\ \sin\left(\frac{\theta_{CM}}{2}\right)\ \cos\left(\frac{\theta_{CM}}{2}\right)$$

$$q\ r\,/\,\hbar c \approx 5\,(q\,/\,1\,\mathrm{GeV/c})\,(r\,/\,1\,\mathrm{Fm})$$

Rutherford scattering:

$$\frac{d\sigma}{dq} = 8\pi\left(\frac{Z_1 Z_2 \alpha\hbar c}{\beta}\right)^2 \frac{1}{|\mathbf{q}|^3} \quad ; \qquad \beta = \frac{p_{CM}}{E_{CM}}$$

Rigid sphere collisions:

$$\frac{d\sigma}{dq} = \sigma_{tot}\,\frac{|\mathbf{q}|}{2\,p^2}$$

Technical Background…

Bubble chamber invented by Don Glaser in 1952. Greater than 10^6 exposures were extremely onerous → only channels with $\sigma > 0.1$ μbarn.

Higher energy accelerators and strong focusing magnets enabled smaller emittance particle beams.

Fast transistors developed in the early ’60s permitted compact 100 MHz electronic logic.

Early Significant Experiments

1963 p-p elastic scattering at large momentum transfersand

Phys. Rev. **138**, B165-B172 (1965)

1965 large-angle π-p elastic scattering at high energies

Phys. Rev. **152**, 1162-1170 (1966)

1966 measurement of π^--p elastic scattering at 180º

Phys. Rev. **164**, 1661-1671 (1967)

1967 elastic p-p elastic scattering at 90º and proton structure

Phys. Rev **159**, 1138-1149 (1967)

1967 π, K, and $\bar{p}$ production in the C-M in high energy p-p collisions

Phys. Rev. **166**, 1353-1364 (1968)

p – p scattering at the AGS

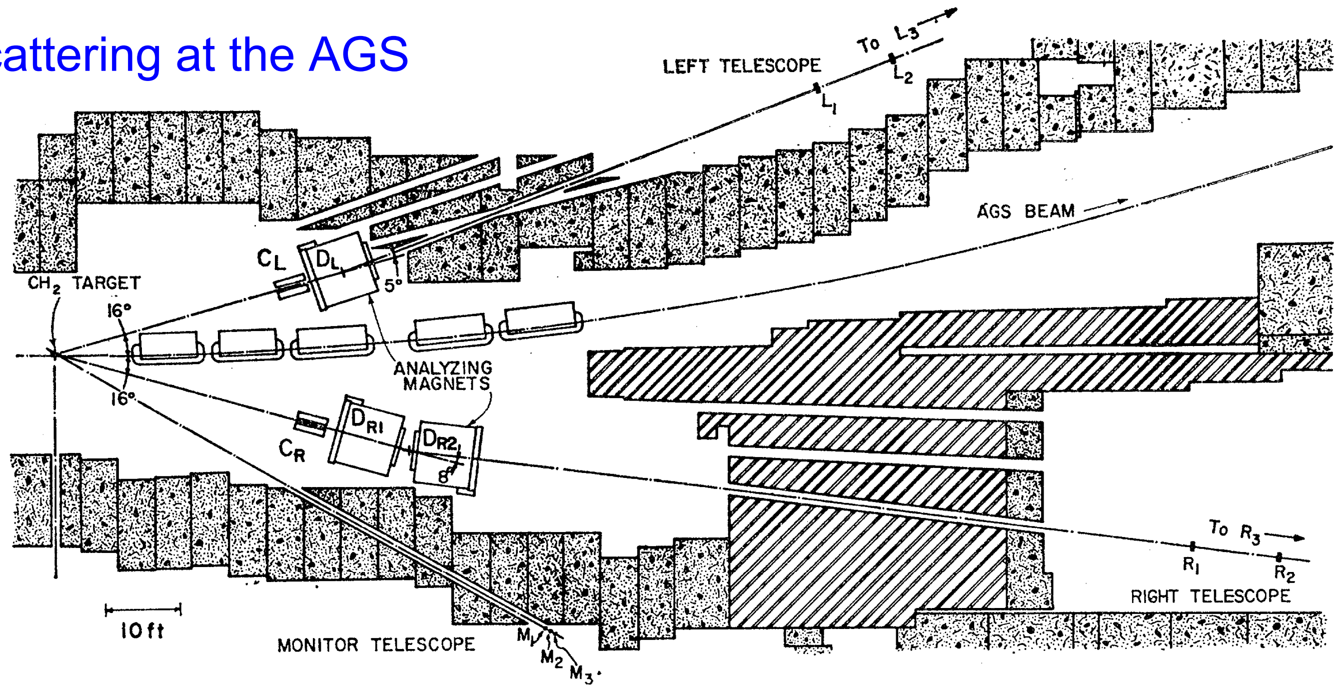

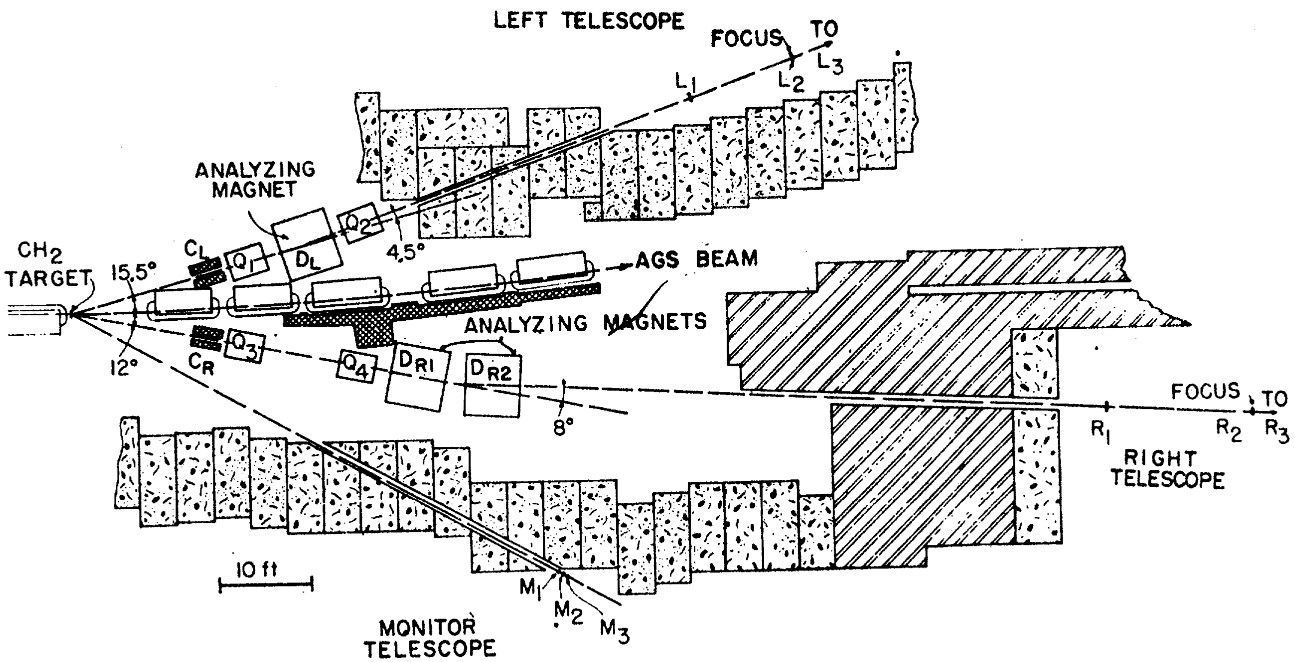

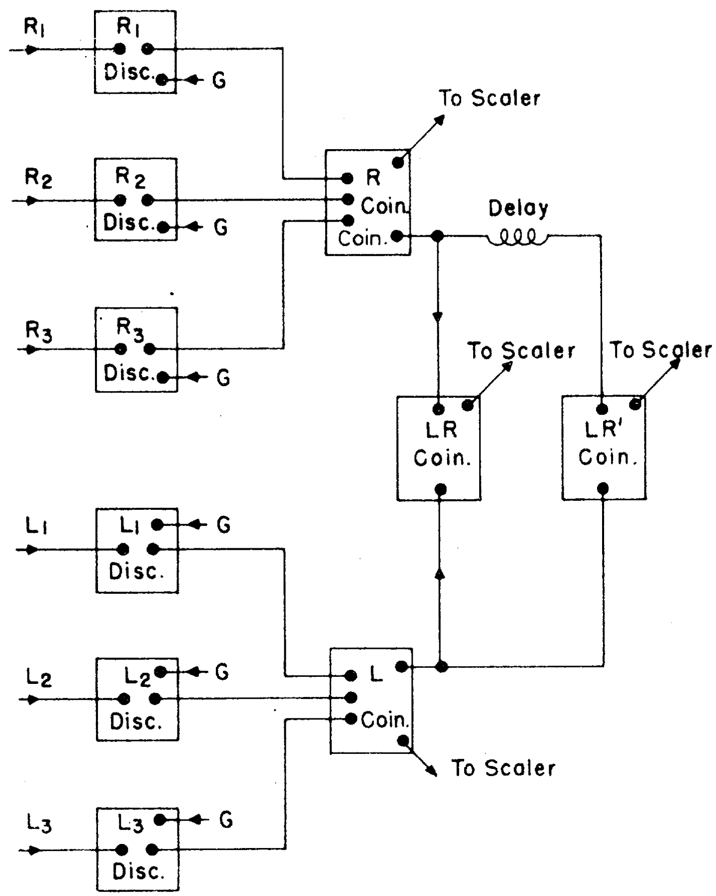

L-R telescopes coincidence logic

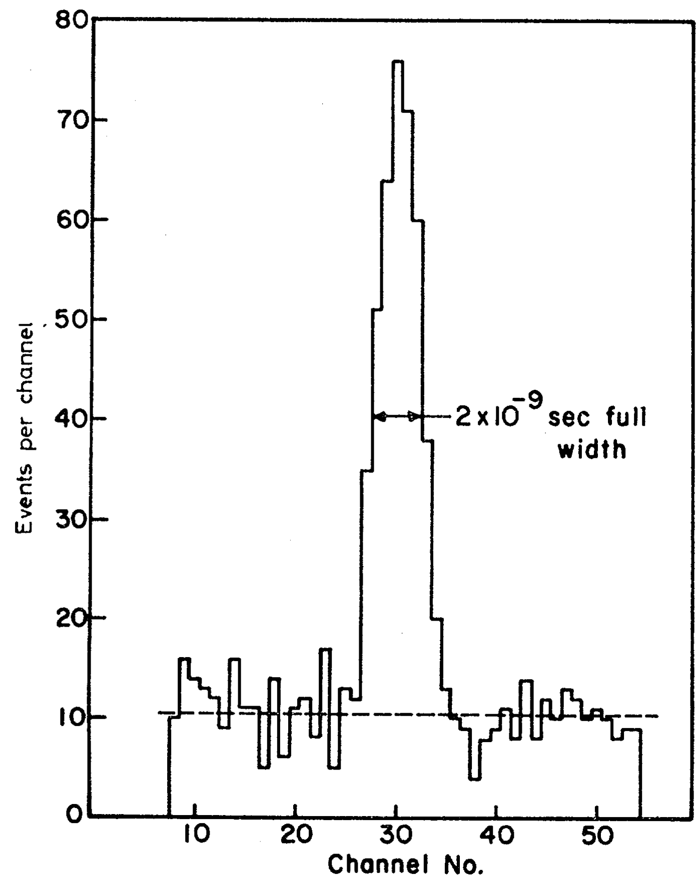

L-R time-of-flight correlation

Some parameters of the AGS p – p elastic scattering experiment

10^{11} protons on internal target, ~100 multiple traversals permit ~10 cm path length in CH_2

$\mathcal{L} \sim 10^{35}$ cm^{-2} s^{-1} (Tevatron ~ 10^{32} cm^{-2} s^{-1})

$\int \mathcal{L}\, dt \sim 10^{40}$ cm^{-2} (one day)

Lowest cross section: $d\sigma/d\Omega_{cm} = 1.1 \times 10^{-36}$ cm^2 sr^{-1}

$d\Omega_{cm} \sim 3 \times 10^{-3}$ sr $\Longrightarrow$ Lowest number of events ~ 25

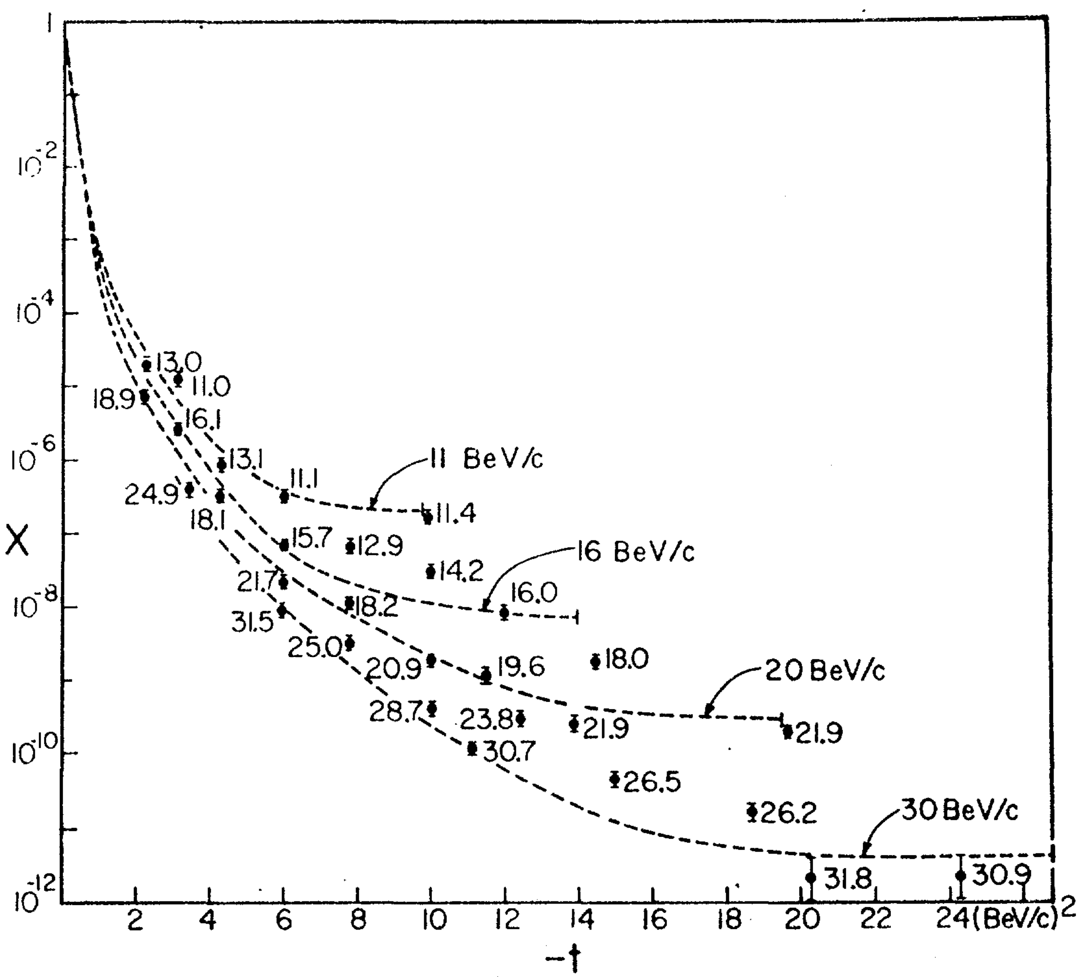

normalized $d\sigma/d\Omega_{cm}$ vs. t

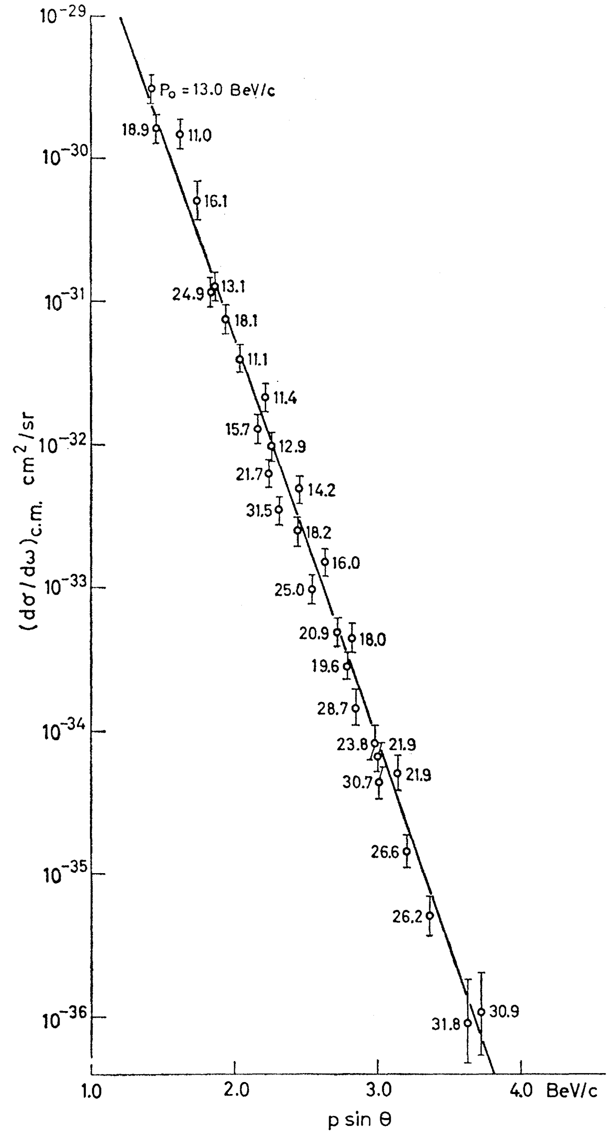

$d\sigma/d\Omega_{cm}$ vs. $p_\perp$

PROTON-PROTON SCATTERING AND STRONG INTERACTIONS*

Alan D. Krisch†
Laboratory of Nuclear Studies, Cornell University, Ithaca, New York
(Received 5 June 1963; revised manuscript received 9 August 1963)

There has recently been considerable interest in the high-energy differential cross section of strongly interacting particles. We will show that for proton-proton scattering the existing data can be fit by a simple function which can be understood in terms of a simple model.

We consider the differential cross section for elastic proton-proton scattering, which is normalized according to

$$X(s,t) = \frac{d\sigma/dt}{d\sigma/dt|_{t=0}^{\text{opt}}} = \frac{d\sigma/d\Omega}{d\sigma/d\Omega|_{\theta=0}^{\text{opt}}}, \qquad (1)$$

where $d\sigma/d\Omega_{\theta=0}^{\text{opt}} = k^2\sigma_{\text{tot}}^2/16\pi^2$.

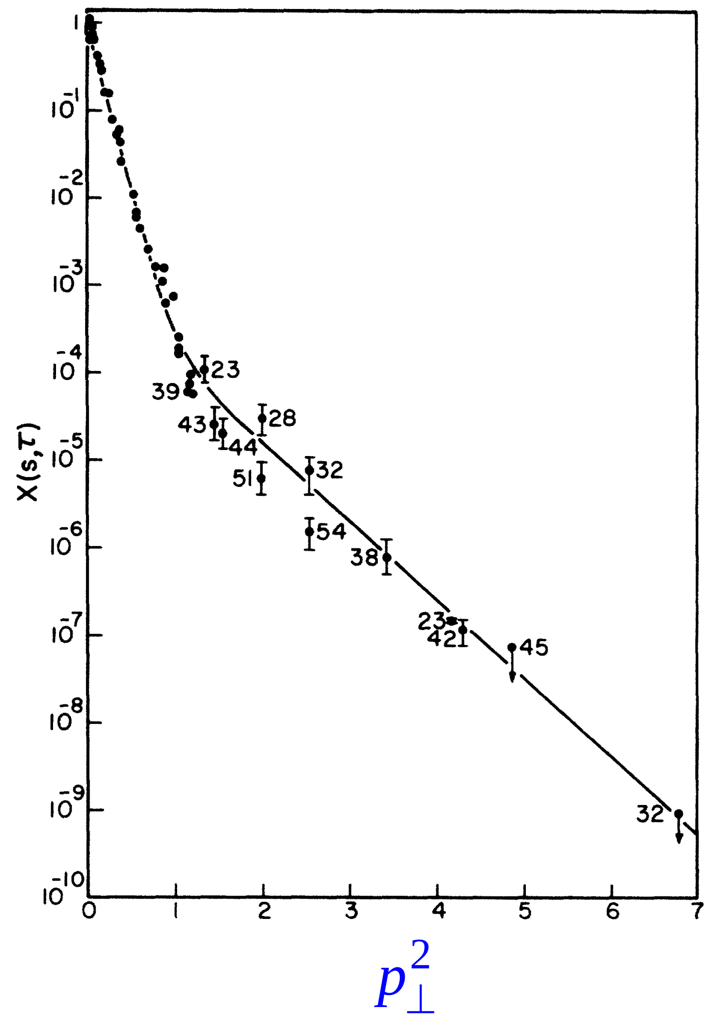

Exponential fit:

$$X(s,\, p_\perp^2) = Ae^{-a\,p_\perp^2} + Be^{-\beta p_\perp^2}$$

π-p elastic scattering at high energies

(8 – 12 GeV/c)

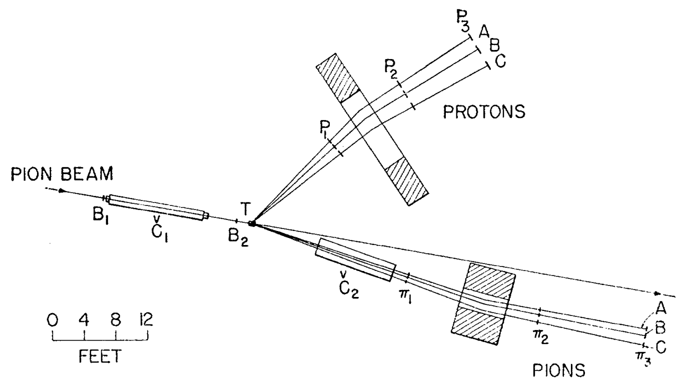

FIG. 3. Layout for Geometry 1. Several different magnet positions were used to obtain different regions of scattering angle.

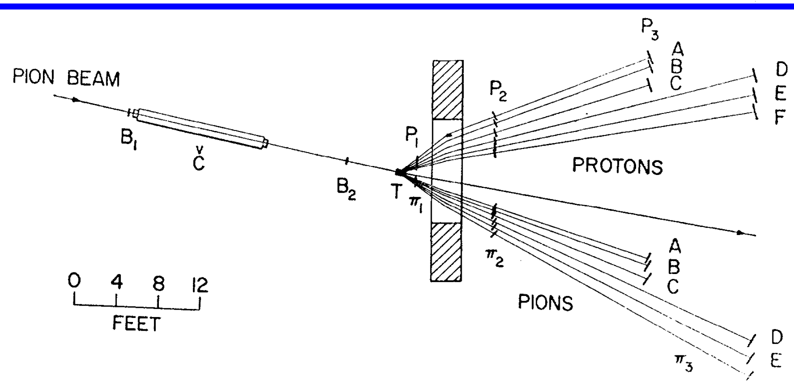

FIG. 4. Layout for Geometry 2 which was used for scattering angles up to 81° in the center-of-mass system.

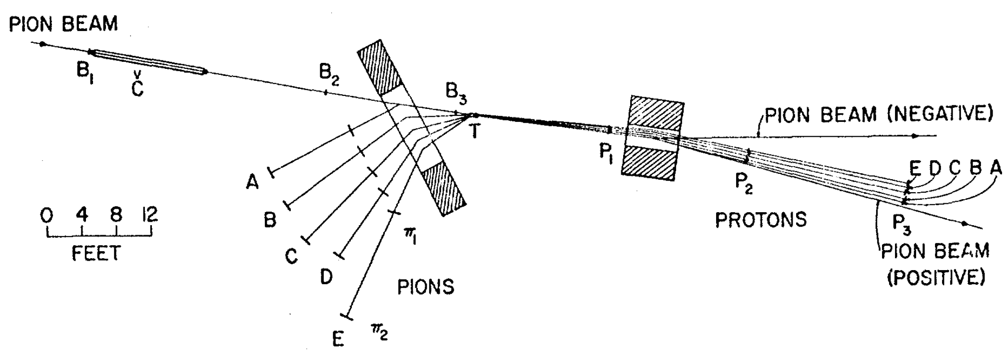

FIG. 5. Layout for Geometry 3 which was used for scattering angles near 180°.

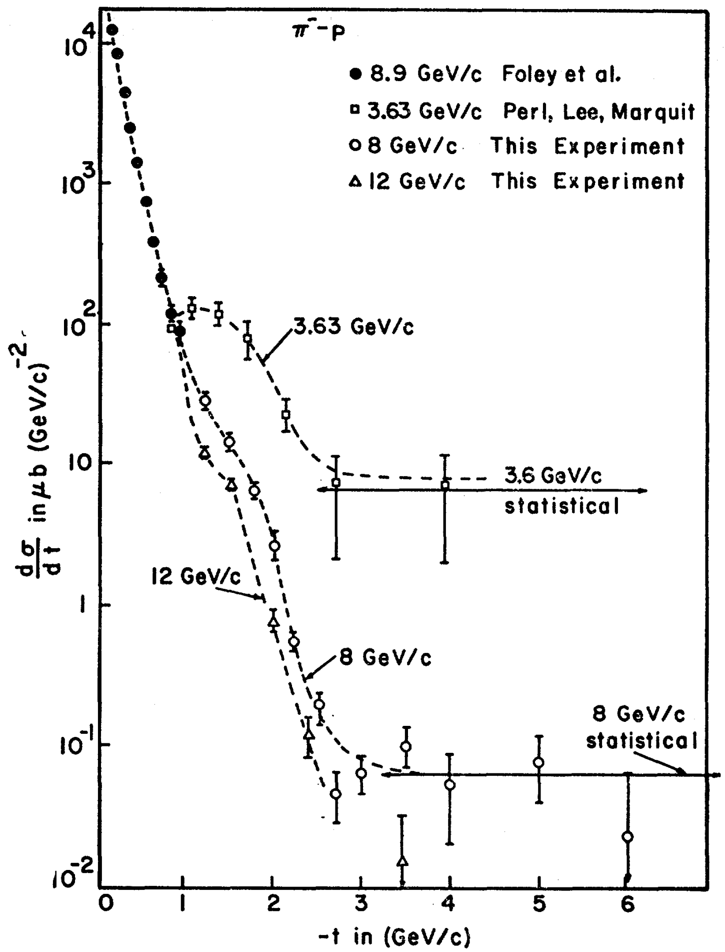

FIG. 6. Angular distributions for π^{-}-p elastic scattering at lab momenta of 3.63, 8, and 12 GeV/c. Curves are drawn only as a guide.

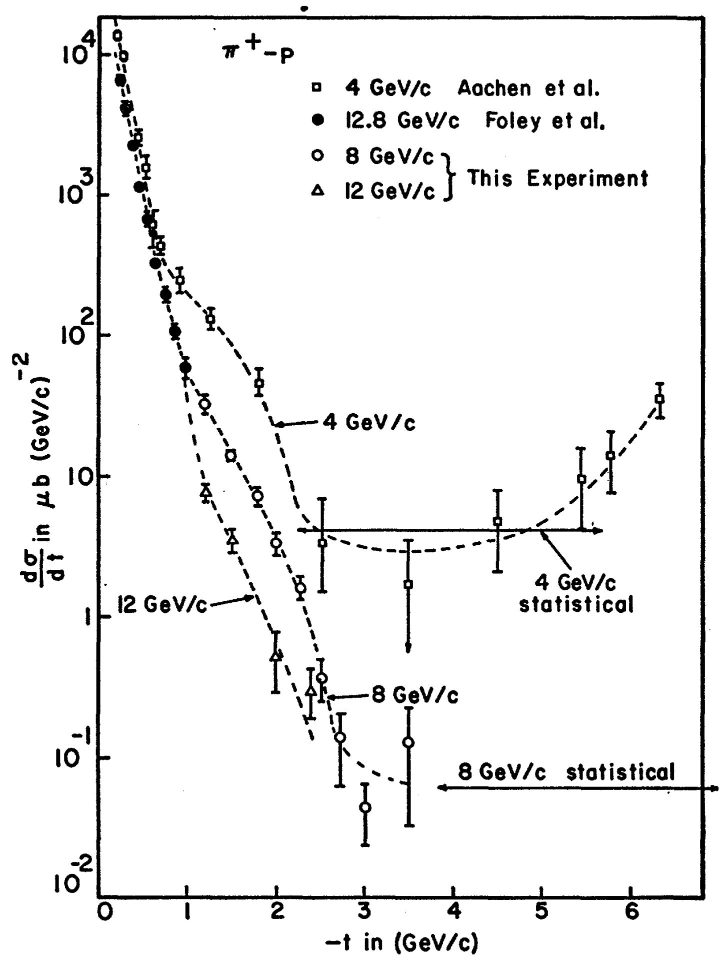

FIG. 7. Angular distributions for π^{+}-p elastic scattering at lab momenta of 4, 8, and 12 GeV/c. Curves are drawn only as a guide.

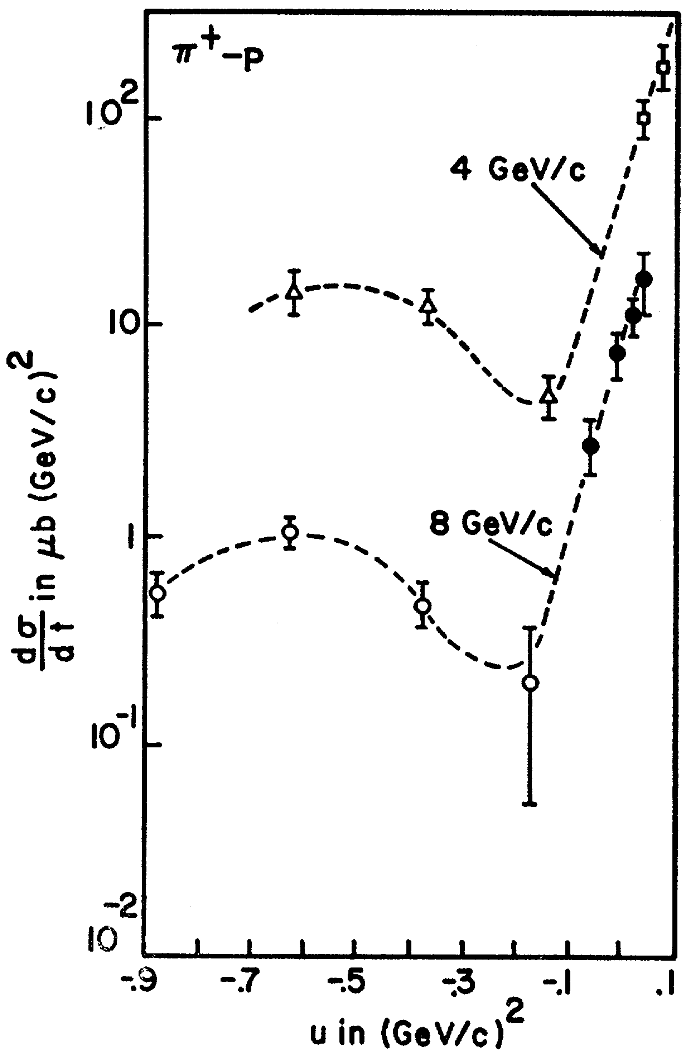

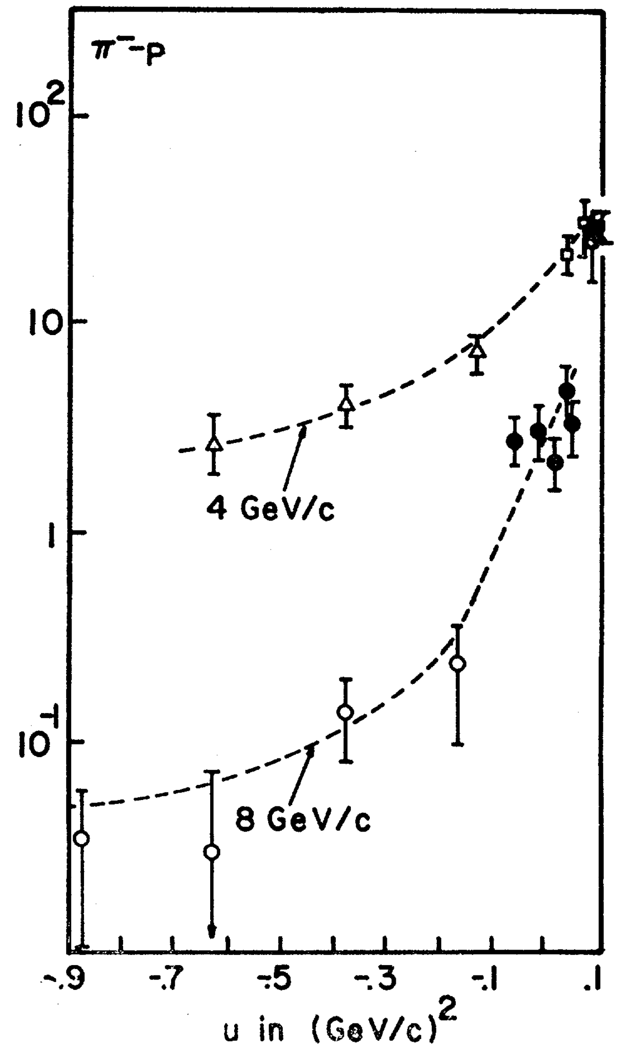

π± - p backward elastic scattering near 180º

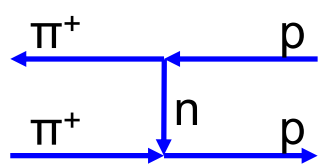

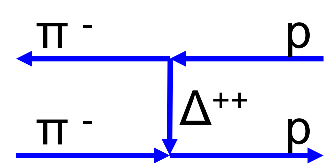

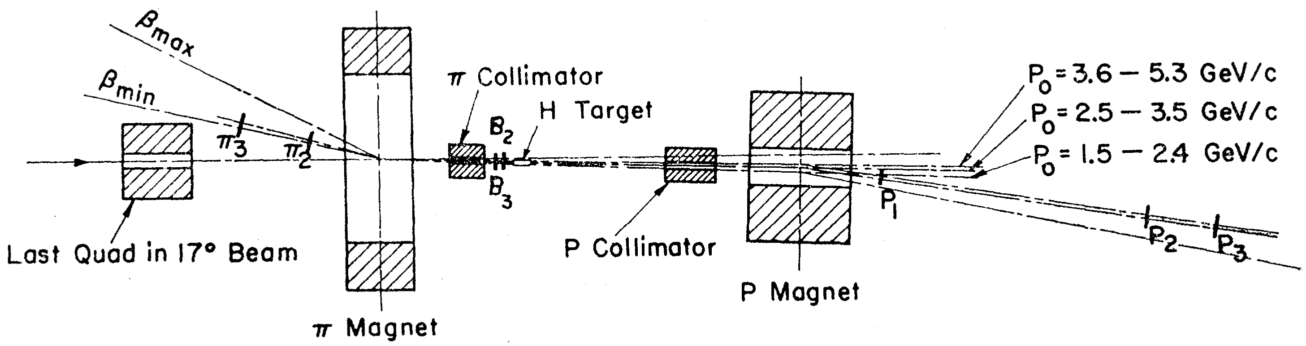

π⁻ - p backward elastic scattering

(1.6 – 5.3 GeV/c)

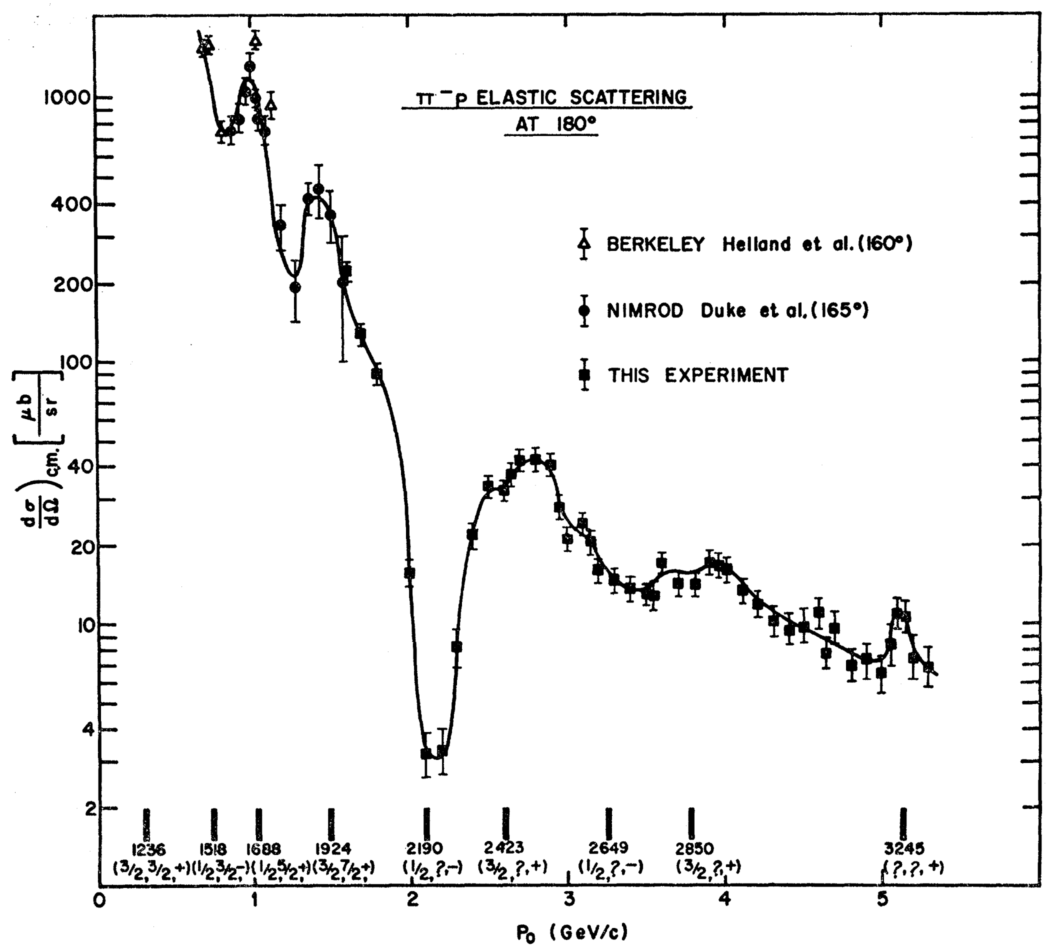

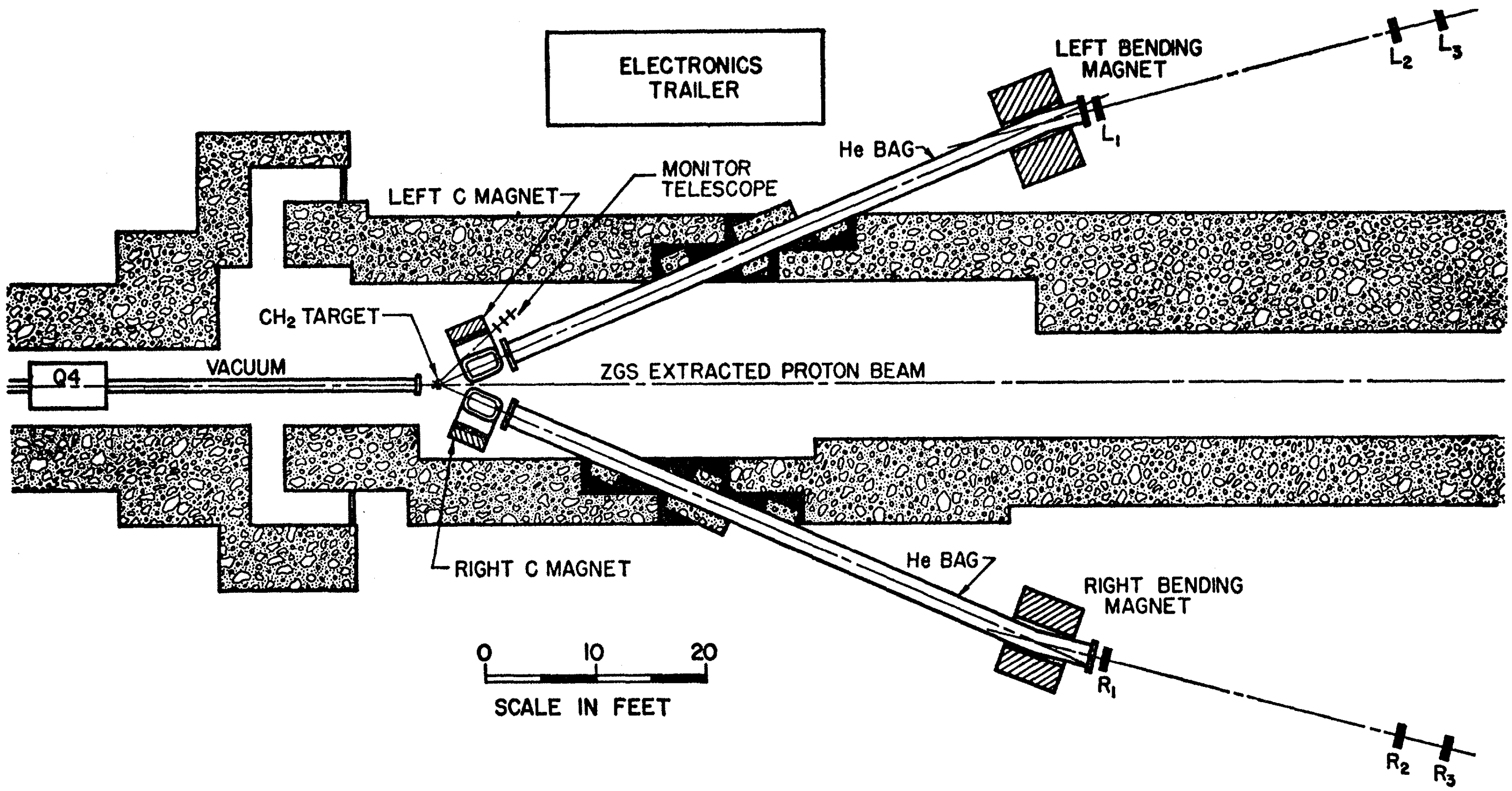

FIG. 3. Experimental layout; the incident protons come down the extracted beam and strike the target. The scattered protons pass out through the magnets and scintillation counters.

elastic p-p scattering at 90° and proton structure

(5.0 – 13.4 GeV/c)

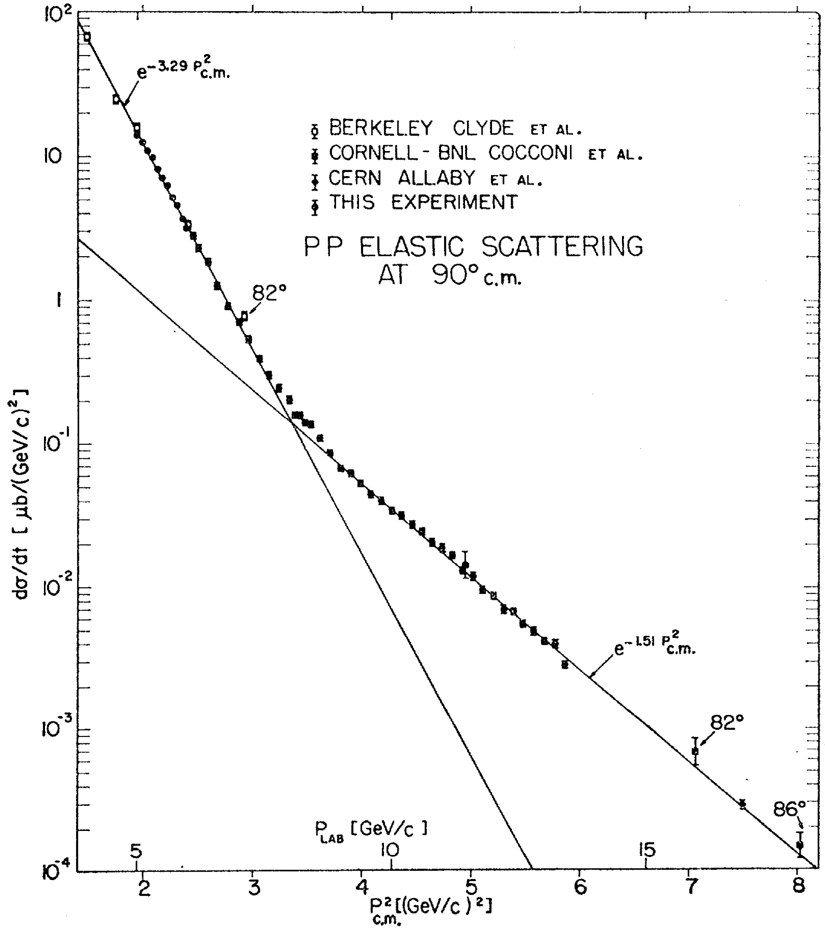

FIG. 8. Plot of $d\sigma/d\Omega$ versus $P_{c.m.}$ for 90° proton-proton elastic scattering. Other data (Refs. 20, 22, 23) are also plotted. The line drawn is the straight line fit suggested by the statistical model.

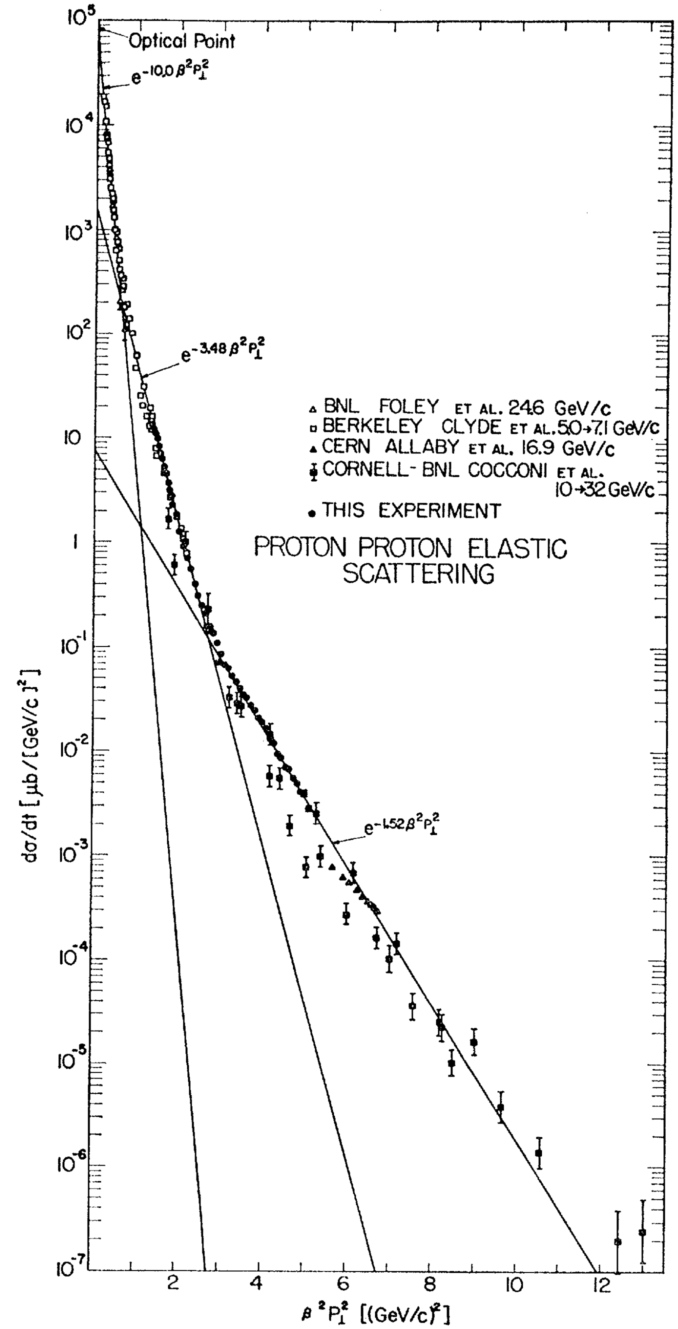

FIG. 10. Plot of $d\sigma/dt$ versus $P_{c.m.}{}^2$ for proton-proton elastic scattering at 90°, comparing it to electron-proton elastic scattering at high momentum-transfer. The lines drawn are the straight line fits to the proton-proton data. The electron-proton data (Ref. 44) are plotted as the fourth power of the form factor, and are normalized to the proton-proton cross section.

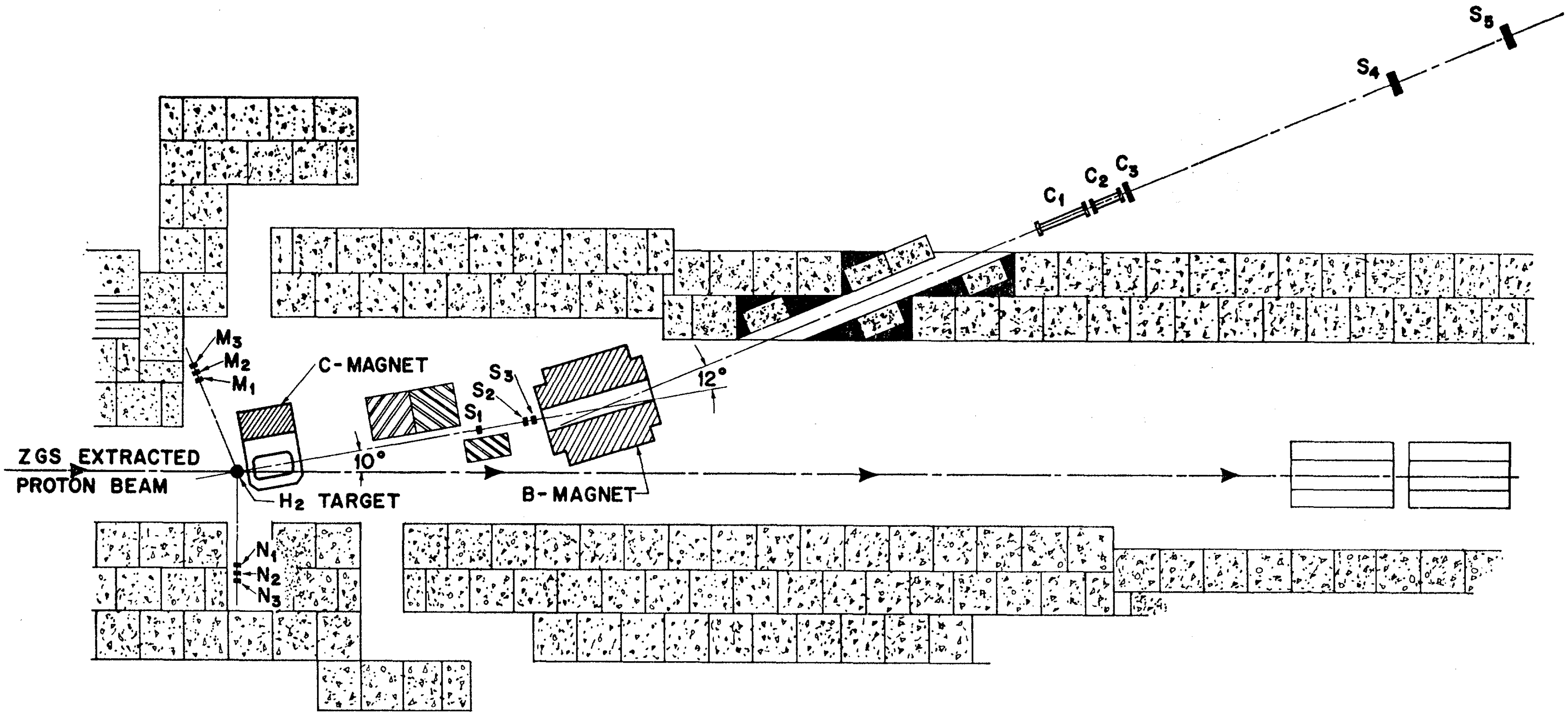

FIG. 2. Layout of the experiment. The incident protons come down the extracted beam and strike the hydrogen target. The produced particles are detected by the spectrometer.

π, K, and $\bar{p}$ production in the C-M in high energy p-p collisions

(12.5 GeV/c)


DO NOT TOUCH

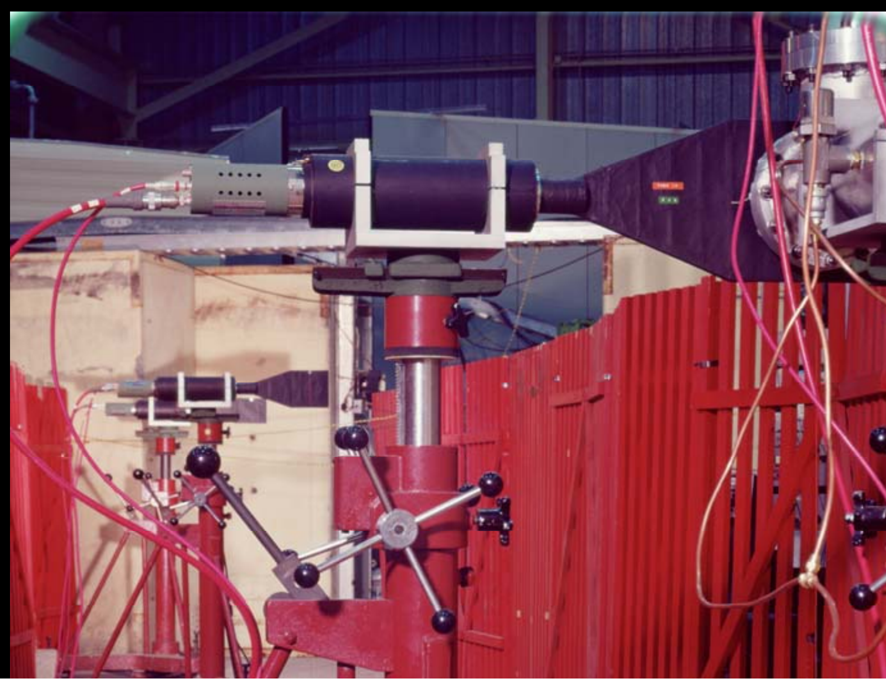

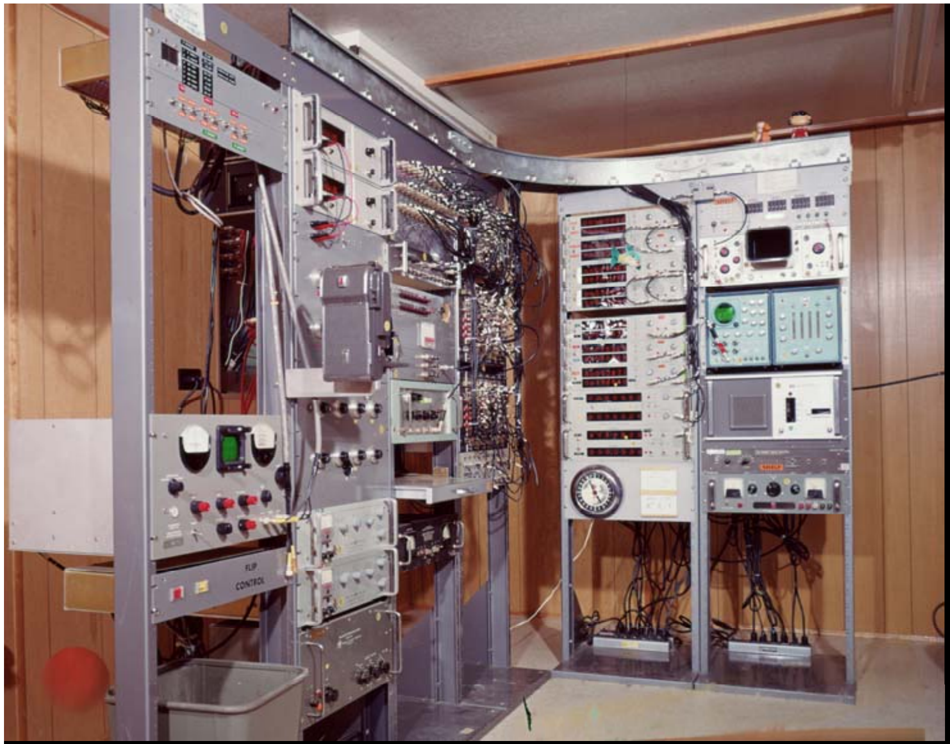

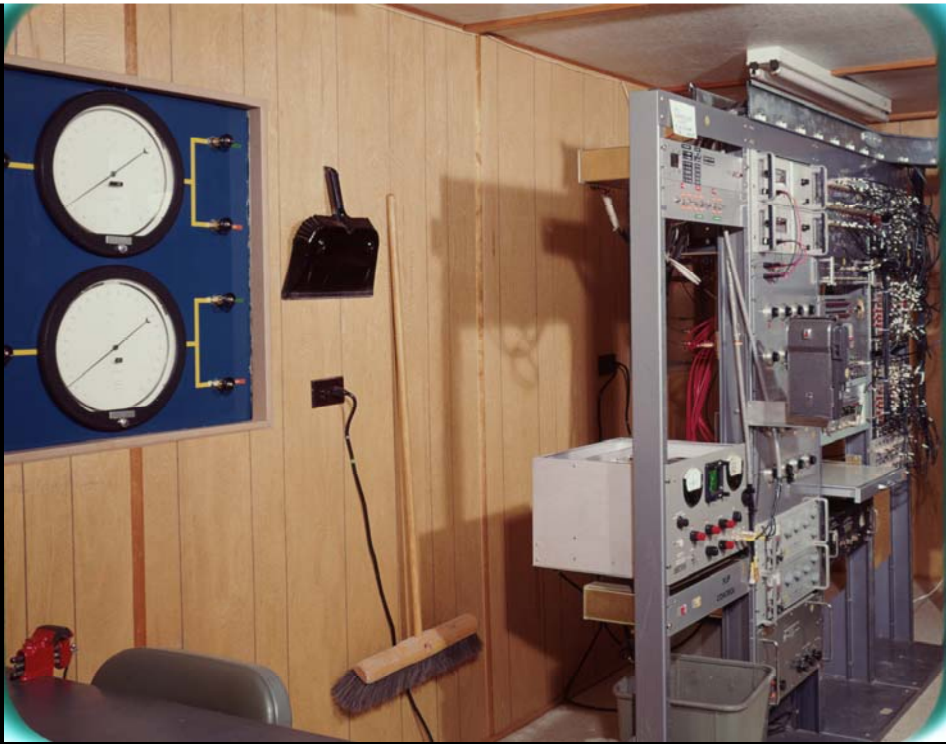

particle production experiment fast logic and controls

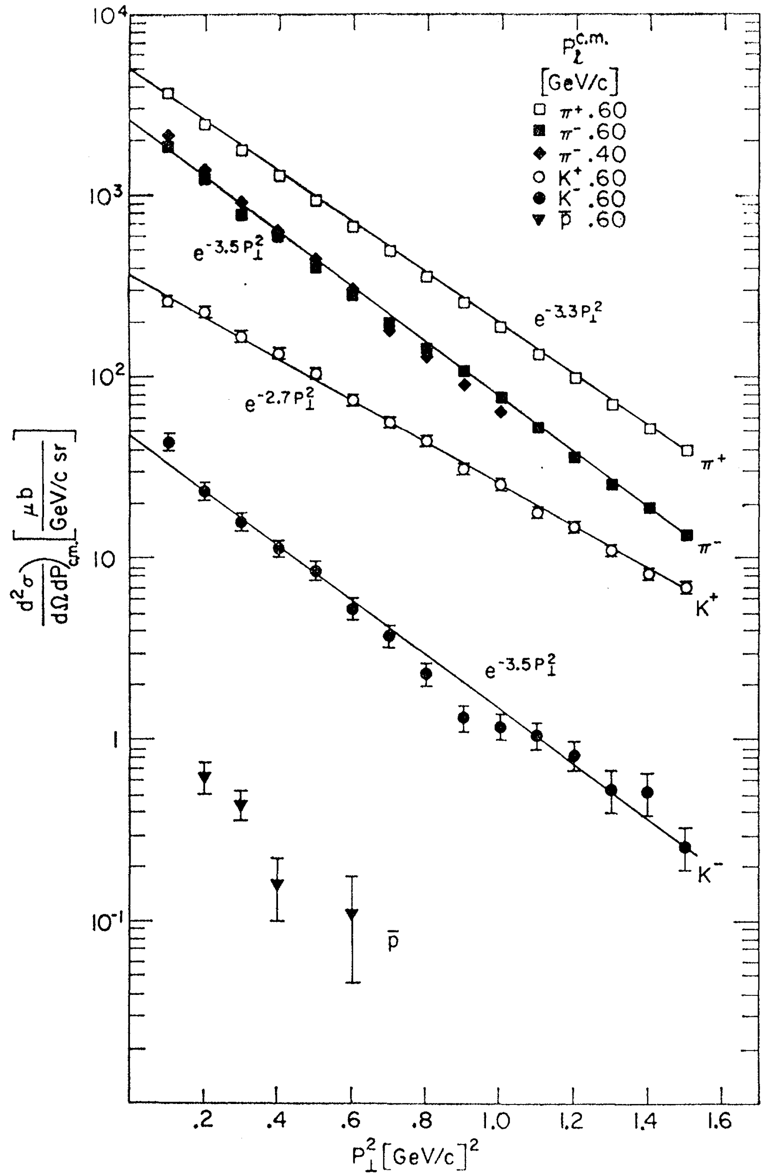

FIG. 11. Plot of $d^2\sigma/d\Omega dP$ against $P_\perp^2$ for $P_l^{c.m.}$ held fixed. The production cross sections for π^+, π^-, K^+, K^-, and antiprotons are shown. The lines are straight-line fits to the data.

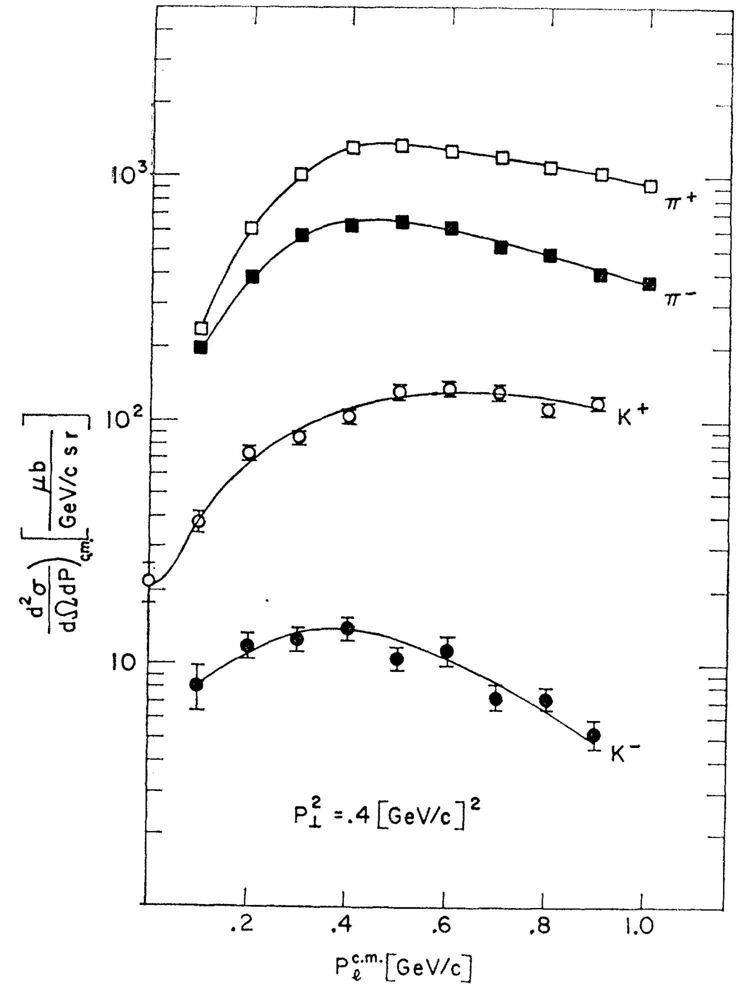

FIG. 12. Plot of $d^2\sigma/d\Omega dP$ against P_l for $P_\perp^2$ held fixed. The cross sections for π^+, π^-, K^+, and K^- production are shown. The lines are freehand fits to the data.

Alan Krisch’s Cornell transportation

All Best Wishes…